Active Magnetic Bearing Systems for Turbomachinery Applications based on Standard Drive Technology

Dr.-Ing. Joachim Denk*
Siemens AG
I DT LD AP SM DW EN 4
Berlin, Germany

Dr.-Ing. Hans-Georg Köpken
Siemens AG
I DT MC R&D 2 2
Erlangen, Germany

Dietmar Stoiber
Siemens AG
I DT MC R&D 2 1
Erlangen, Germany

Frank Viering
Siemens AG
I DT MC R&D 2 1
Erlangen, Germany

Abstract

Around two decades ago, active magnetic bearings (AMB) were introduced into O&G-applications (Oil & Gas- applications), but never gained any relevant market share in large turbomachinery. This paper discusses how standard drive technology from machine tool applications can be used to control AMB systems and how the integrated data acquisition functions simplify the commissioning process. As a proof of the concept, results of prototype testing with a 5 MW induction motor are presented.

1 Introduction

Active Magnetic Bearings (AMBs) have been used in the O&G industry for more than 20 years. The advantages of AMBs in O&G-applications are obvious: oil-free, clean, small footprint as direct drive systems can be used, low vibration and a wide operational speed range.
However, despite these convincing advantages, the technology did not make any breakthrough, and the number of new projects with AMB technology in O&G applications remains stable but small. Key limiting factors are:

1. Limited customer confidence, since comprehensive data about reliability and availability of the drive components of an AMB system is not readily available for specialized AMB hardware, which is typically manufactured in small numbers.
2. Restricted network of service and commissioning personnel of the AMB supplier, as only a small quantity of specialized AMB drive hardware is sold.
3. The limited number of experts at the end user, who are familiar with specialized AMB drive hardware.

These restraints can be overcome over the long term by gradually building up customer confidence and establishing specialized AMB hardware as a mass product in the market. However, this process can be significantly accelerated if drive technology can be successfully applied to AMBs, which is built more than a 100,000 times a year, and which is already a proven and accepted technology in a different, but closely related field: standard drive controllers and power modules for machine tool applications.

In this way, AMB technology immediately benefits from highly-industrialized electronic components, the global network of experts and service, the worldwide availability of spare parts and from the proven statistics of standard drive technology components in terms of MTBF.

This paper will show why standard drive hardware is suitable as basis for implementing AMB applications and that only minor software modifications are necessary. The paper explains why the integrated data acquisition

*Contact Author Information: joachim.denk@siemens.com, Siemens AG, I DT LD AP SM DW EN 4, Dr. Joachim Denk. Nonnendammallee 72, 13629 Berlin, Germany

functions simplify the commissioning process. Results of prototype testing with a 5MW induction motor will be presented as proof of the concept.

2 AMB Fundamentals

The basic principle of active magnetic levitation is shown in Figure 1. A ferromagnetic rotor is located in the earth's gravitational field. The deviation of the rotor from a setpoint position is measured by a displacement sensor. A controller converts this information into a current setpoint for a power amplifier. The power amplifier in turn drives the coil of an electromagnet. If the controller is appropriately parameterized, the rotor will levitate. Since a magnet can only exert pulling forces on ferromagnetic bodies, a second magnet located below the rotor is required, if the rotor needs to be actively pulled in the negative x-direction. The two electromagnets together with the sensor form one axis of an AMB.

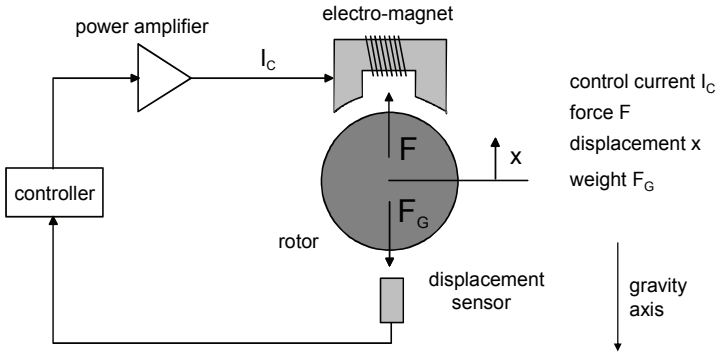

Figure 1: Basic principle of active magnetic levitation

For magnetic levitation of a complete rotor, 5 bearing axes are required, see Figure 2: One radial bearing with two bearing axes at the drive end (DE) of the rotor and one radial bearing at the non drive end (NDE), respectively. One additional axial bearing is required if thrust forces have to be handled. This means that 5 of the 6 degrees of freedom of the rotor are fixed and only the rotational degree of freedom around the z-axis remains.

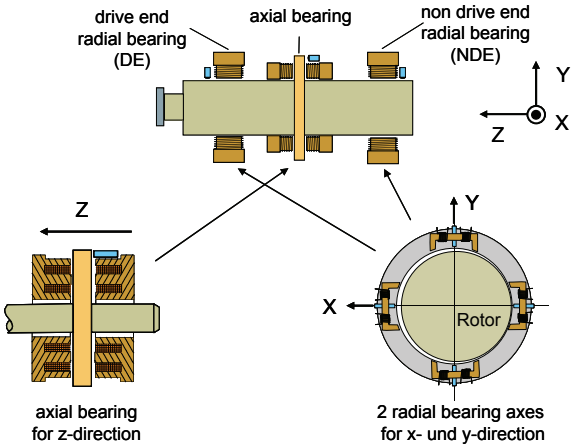

Figure 2: Axes of an AMB-rotor

In a motor-compressor drive train, the motor and the compressor are usually connected through a coupling which is radially compliant but axially stiff, so that only one element requires an axial bearing – typically the compressor. In addition to the magnetic bearings, each axis is equipped with a back-up bearing to support the rotor when the AMB is shut off and to ensure a safe rundown, e.g. in case of a power failure. A back-up bearing is typically realized using a conventional bearing (roller bearing, journal bearing) with an increased bearing gap, so that the rotor is not in contact with the bearing while it is levitated.

3 Operation of AMBs with Standard Drive Technology

Standard drive hardware is used in machine tool applications, for example, to control a torque motor or a linear motor. As illustrated in Figure 3, the idea of using this hardware to realize active magnetic levitation is quite straightforward: A torque motor is very similar to a magnetic bearing stator, as it also consists of coils and laminations. Furthermore, controlling a linear motor to a fixed setpoint position is similar to controlling a rotor in a magnetic bearing.

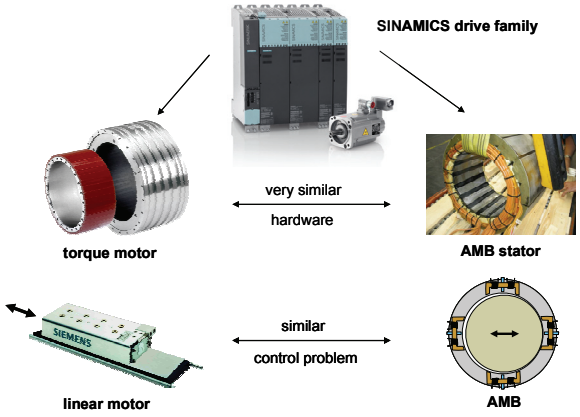

Figure 3: AMB and machine tool applications– parallels

Of course, actuation of a magnetic bearing is not identical to the actuation of a torque motor, the sensor concepts are different and the system dynamics of an AMB differ from those of a linear motor. Thus, the software must be appropriately adapted, which will be explained in the following subsections.

3.1 Sensor Concept and Coupling

A position sensor commonly used in AMB applications is the eddy current sensor. This supplies an analog voltage signal that is proportional to the rotor displacement. Usually, two sensors are installed per axis in the differential mode so that certain disturbances, which act on both sensors in the same way (rotor growth, temperature drift), can be compensated, see Figure 4.

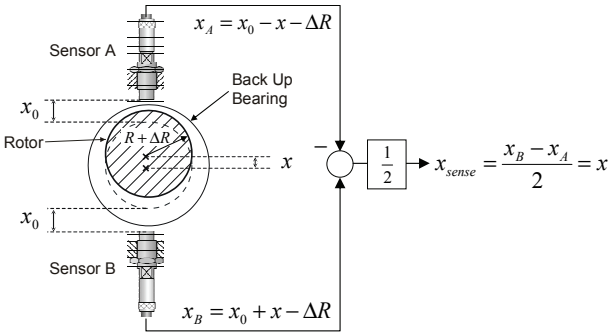

Figure 4: Evaluation of two position sensors in the differential mode at rotor with rotor growth ΔR.

In linear motor applications, however, the position of the motor is typically measured using optical linear encoders as illustrated in Figure 5. An optical grid is scanned by a photo-optical device, which in turn supplies a sine and a cosine signal (trace A and trace B). The number of signal periods is counted and this represents the number of gridlines passed and thus the distance traveled (rough position information). The evaluation of the actual signal amplitude provides the actual position within one gridline (fine position information), where the amplitude is typically sampled with an A/D converter with a resolution of 10-16 bit.

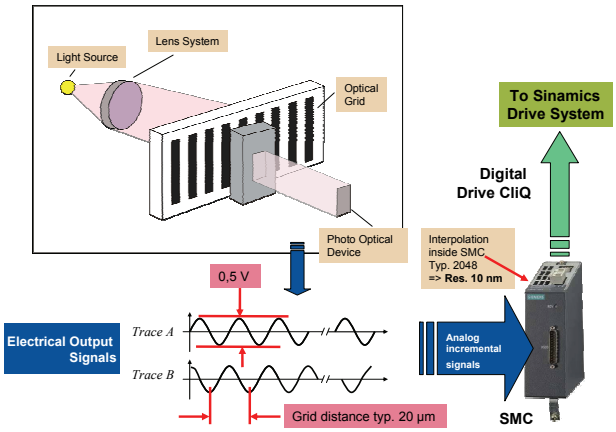

Figure 5: Position measurement in machine tool applications using a linear scale.

Despite these obvious differences in the sensor concepts, the same hardware to evaluate a sine/cosine-encoder can be used to read the analog displacement sensors. This is because the A/D converters used to read the sine-trace A and cosine-trace B are also suitable for reading the analog signals of the eddy-current sensors A and B. Of course, the post-processing to calculate a single displacement signal from the two input signals is different, and thus the software must be modified.

3.2 Actuation of an Active Magnetic Bearing Axis

As pointed out in Section 2 , two electromagnets are required in one bearing axis, if forces on the rotor need to be actively exerted in the positive and negative axis-directions. A straightforward strategy to operate the two coils would be to supply the upper coil with current if the rotor needs to be pulled in the positive x-direction and to supply the lower coil with current, if the rotor needs to be pulled in the opposite direction. However, the relationship between the current and force of an electromagnet is quadratic. This results in a non-linear relationship between current and force, which is a problem for a linear controller (Figure 6).

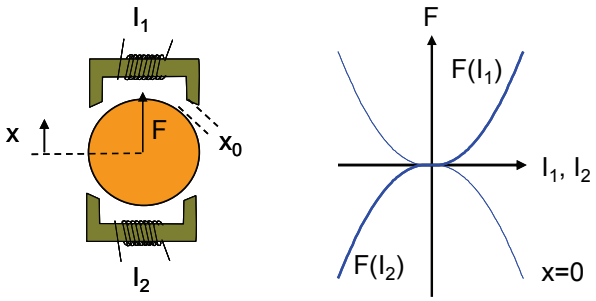

Figure 6: Inappropriate control strategy for AMB coils: $I_1>0$, $I_2=0$ for $F>0$ and $I_1=0$, $I_2>0$ for $F<0$.

To avoid this non-linearity in the current/force relationship, conventionally, a constant bias current I_0 is applied to both coils. To exert a positive force on the rotor, current I_1 in the upper coil is increased by the control current I_C - while the current in the lower coil I_2 is decreased by current I_C – and vice versa for negative forces. As a consequence, two quadratic functions are added, which result in the linear current to force relationship shown in red in Figure 7, when the rotor is in its setpoint position x=0:

$$F = k \cdot \left(\frac{I_0 + I_C}{x_0 - x} \right)^2 - k \cdot \left(\frac{I_0 - I_C}{x_0 + x} \right)^2 \Bigg|_{X=0} = \underbrace{\frac{k}{x_0^2} \cdot 4 \cdot I_0}_{K_I} \cdot I_C \tag{1}$$

where k is a constant. K_I is the force per control current constant of the bearing.

However, two two-phase inverters are required to operate a magnetic bearing axis, since unequal currents are required in the upper and lower coils.

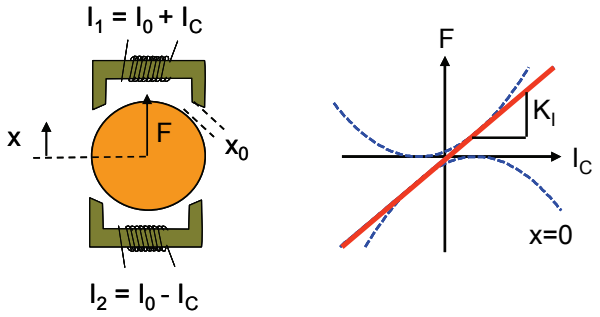

Figure 7: Conventional control strategy for AMB coils: Constant bias current I_0 and control current I_C.

Standard inverters in machine tool applications are used to drive three-phase AC motors. Thus, they are able to drive a current in three phases. Needless to say, two three-phase inverters could be used to realize the conventional control strategy shown in Figure 7. However, one phase in each inverter would remain unused and the hardware would not be used to its full capability. To avoid this, a method was created, which allows a complete magnetic bearing axis to be operated with a single three-phase inverter. This is achieved using a simple modification in the drive software.

The basis for this method is the field oriented control for three-phase motors implemented as standard in the drive software. Field-oriented control for three-phase motors relies on the Clarke-Park-transformation, which depends on the actual angular position of the rotor and relates the torque current i_q and the flux current i_d to the phase currents i_R, i_S and i_T. The current i_d is only required in motor applications in the case of field weakening and is usually controlled to a value of zero. Current i_q is proportional to the force/torque delivered by the motor. The Clarke-Park-transformation allows the flux current i_d to be independently controlled from torque current i_q for arbitrary rotor positions. For a rotor angle of zero, the Clarke-Park-transformation yields

$$\begin{aligned} i_R &= i_d &&= -2 \cdot I_0 \\ i_S &= -\frac{1}{2} i_d + \frac{\sqrt{3}}{2} i_q &&= I_0 + I_C \\ i_T &= -\frac{1}{2} i_d - \frac{\sqrt{3}}{2} i_q &&= I_0 - I_C \end{aligned} \qquad (2)$$

These equations show that flux current i_d influences the current in phases S and T in the same way, and torque current i_q increases the current in phase S while it decreases the current in phase T. If the magnetic bearing coils are connected to the inverter as shown in Figure 8, current i_S flows through the upper coil and current i_T flows through the lower coil. If i_d is chosen to be $i_d = -2\ I_0$ and i_q is chosen to be $i_q = 2/\mathrm{sqrt}(3)\ I_C$, then the complete bearing axis can be operated using just one servo inverter.

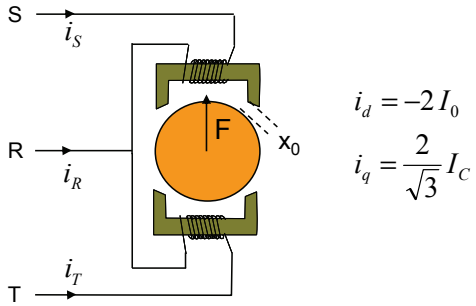

Figure 8: New control strategy – one three-phase inverter provides control current I_C and bias current I_0.

3.3 Controller Concept for AMB Applications

In addition to the software modifications needed for sensor and actuator coupling as described in the preceding two subsections, modifications to the control algorithm are required because of the distinctive features of the magnetic bearing plant dynamics. This fact is going to be explained by comparing the plant dynamics of a linear motor with a magnetic bearing axis.
As long as friction and compliant elements are neglected in a linear motor axis, the dynamics of the linear motor axis can be modeled as a double integrator, see Figure 9. Thus, the machine table M will either remain stationary or it will travel with a constant velocity v - assuming that no force F is applied to the table by the linear motor.

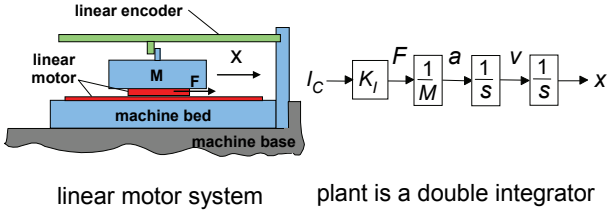

Figure 9: Plant dynamics of a linear motor axis.

On the other hand, the plant dynamics of the simplified AMB axis shown in Figure 10 (left) are unstable. This is due to a negative stiffness K_X of the electromagnetic actuator in the bearing axis: As seen in (1), in addition to the control current I_C , the actuator force also depends on the rotor position x. This is due to the fact that the magnetic flux increases with decreasing air gap. If (1) is evaluated for constant control currents I_C, the set of characteristic curves in Figure 10 (right) is obtained. The diagram shows that a small movement of the rotor in the positive direction for a constant control current I_C leads to an increasing force in the same direction, which further accelerates the rotor, see Figure 10 (left). This behavior means the plant is unstable and the linearized relationship between position and force in the setpoint is called negative stiffness K_X.

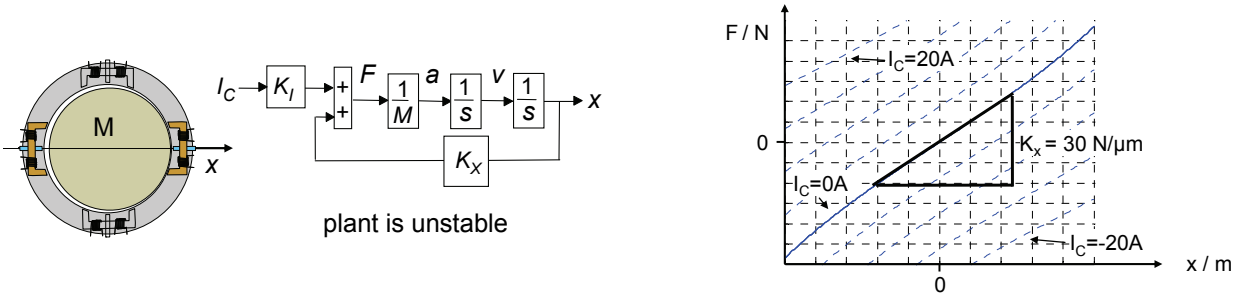

Figure 10: Plant dynamics of a simplified AMB axis (left). Relationship between force F and position x for different control currents I_C , i.e. negative stiffness K_X (right).

However, the plant instability can be easily compensated using a simple PID controller, see Figure 11. When the force constant K_I of the magnetic actuator is compensated by a factor of $1/K_I$ in the controller, the following relationship is obtained between force as a result of controller action f_C and rotor position x for a constant setpoint position x_S of zero:

$$f_C(s) = -K_P \cdot \left(1 + \frac{1}{T_N \cdot s} + T_V \cdot s\right) \cdot x(s) \tag{3}$$

Obviously, the proportional part of the controller K_P feeds back the rotor position, generating a negative force; while the negative stiffness of the actuator K_X, feeds back the rotor position generating a positive force. Thus, as long as K_P is chosen larger than K_X, the resulting stiffness is positive and the system can be stabilized.

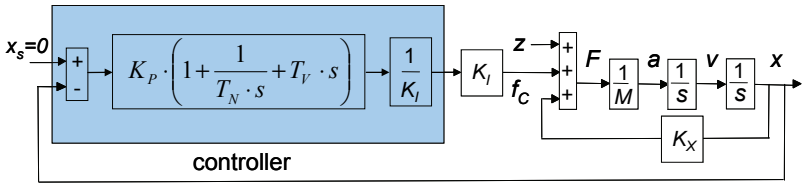

Figure 11: Simplified control loop for an AMB axis (current controller, time delays and filter elements are neglected).

Apart from the proportional part K_P, the derivative action T_V allows damping to be introduced into the system, while the integral action time T_N is only required to avoid static deviations from the setpoint position x_S in case of disturbances – such as the force of gravity.

In machine tool applications, however, the standard controller is a cascaded control structure with an inner velocity control loop and an outer position control loop [1]. This cascaded control loop allows axis velocities to be effectively limited, which is however not required in AMB applications. Although the cascaded control structure can be used to stabilize an active magnetic bearing axis in principle, the parameterization of the control parameters is less intuitive. Thus, a PID control algorithm is implemented in the drive software instead.

3.4 Human-Machine-Interface, Supervision and Communication

The following important high-level functions are required in magnetic bearing motor applications:

1. *Process Supervision:* continuous supervision of bearing positions, currents, voltages and temperatures
2. *Communication:* hand-shake with the motor inverter, e.g. immediate braking command in case of alarm messages, interface to the internet for remote monitoring and operation.
3. *Operator Panel:* activation and deactivation of the AMB, definition of warning and alarm levels
4. *Fault Diagnosis:* fault buffer, trip database

This functionality, along with additional functionality to simplify commissioning and fault diagnosis, can be easily realized with an appropriate user program running on a higher-level standard motion control system, see Figure 12 for an overview of the resulting complete system.

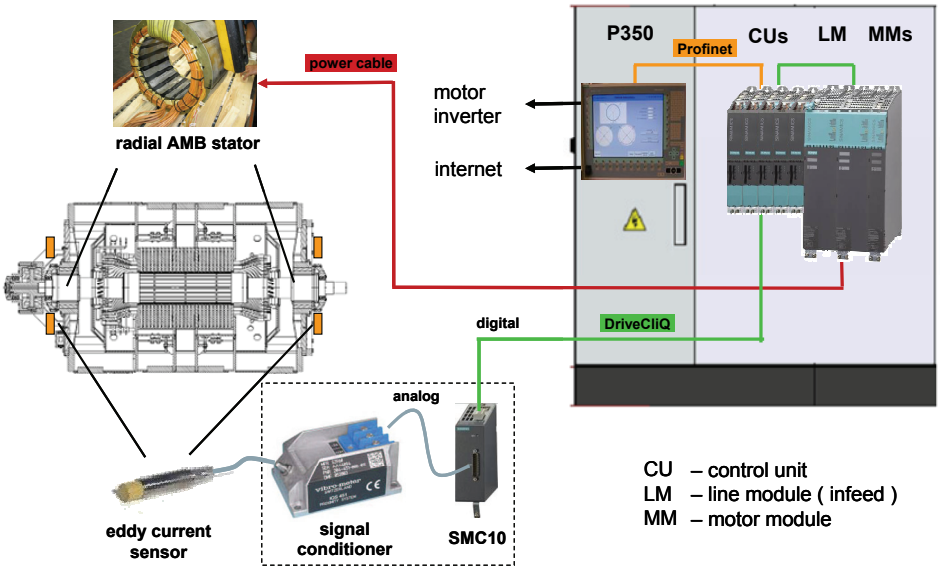

Figure 12: Overall AMB system based on standard drive technology.

4 System Dynamics and Controller Parameterization for an AMB Motor

A detailed discussion on the system dynamics of AMB applications and on the controller parameterization is not the focus of this paper. Instead, an overview is given on the underlying principles, which are essential for the interpretation of the experimental results that will be subsequently explained. As indicated, plant and controller dynamics are simplified for the considerations in Figure 10. In reality, the rotor is not stiff but compliant, being able to perform bending vibration. Furthermore, the underlying current controller, the sensor dynamics and time delays introduce phase loss into the open loop system.

The first three bending modes resulting from an FEM calculation for the rotor of the 5 MW, 13000 rpm test motor with a solid shaft are shown in Figure 13. While mode shapes and bending frequencies can be predicted with a high accuracy using FEM calculations, the viscous damping must be determined using experimental modal analyses. Typically, the modes are very poorly damped with damping values of approximately 0.1%.

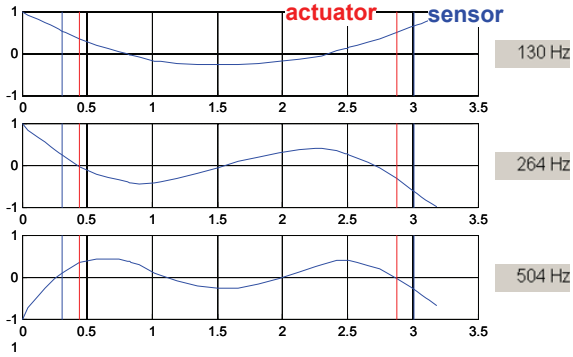

Figure 13: First 3 bending modes of the 5 MW test motor.

Because of the poor damping, the bending modes can be easily excited by unbalance forces, if the rotor speed is close to the bending frequency or if the bending frequency even needs to be passed through. In such cases, the vibration amplitude of the rotor can become so high that the rotor comes into contact with the back-up bearing. To prevent this, the controller must supply sufficient damping to bending modes in or close to the operational speed range. To operate the rotor at a speed coinciding with a bending frequency, API Standard 617 stipulates a damping ratio of greater than 20% (amplification factor AF less than 2.5) [3].

Bending modes appear as resonances in the open position control loop. Whether a particular resonance can be damped by the controller, depends on the controller gain and phase at that frequency and on the position of the nodes of the bending mode with respect to actuator and sensor positions [2]. If the gain and phase are inappropriate and the Nyquist stability criterion is not met, the controller can even destabilize a mode. In such a case, gain and phase need to be shaped by applying filters.

The required filters (PT1, PT2, general 2^{nd} order filter) are also used in machine tool applications, for example, if a resonance caused by a compliant element in the force transmission path of a machine tool axis limits the controller amplification and thus the system bandwidth [1]. Filters and tools for filter parameterization have already been implemented in the standard drive software because of this effect. However, because of higher bandwidth requirements in AMB motor applications and a stronger influence of actuator and sensor positions on the controller performance, the filter design is considerably more challenging in AMB applications than it is in machine tool applications. Furthermore, bending frequencies depend on the rotor speed because of gyroscopic effects, making it necessary to verify the controller performance over the complete operational speed range.

The influence of the rotor speed on the first two bending modes of the test rotor is illustrated in the Campbell diagram of the system, see Figure 14 (left). In a Campbell diagram, bending frequencies are plotted versus rotor speed. It can be seen, that due to the gyroscopic effects, the bending frequencies split into an upper branch (forward bending mode) and a lower branch (backward bending mode). For a well behaved motor design, only forward bending modes can be excited by unbalance. The speeds at which the rotor speed coincides with the frequency of the

forward bending modes (intersection between run up beam and upper branches), are called the critical speeds. To reach the maximum operational speed of 13,000 rpm, the test motor needs to pass through one bending mode.

When the control loops of the AMBs are closed, introducing stiffness and damping at the bearing locations, the rotor can exert translational and tilting vibrations (rigid body modes) in addition to bending modes. Rigid body modes can also be excited by unbalance and require proper damping. The Campbell diagram in Figure 14 (right) shows an example for a particular controller parameterization, where the frequencies of the two rigid body modes are clearly separated from each other.

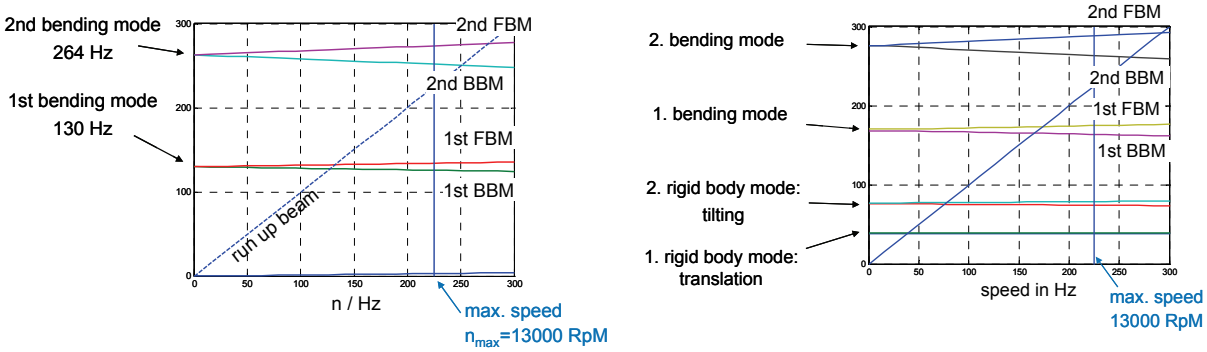

Figure 14: Campbell diagram of the **free-free-rotor**, with forward (FBM) and backward bending modes (BBM) (left). Campbell diagram of a **controlled rotor** with rigid body modes for a particular controller setting (right).

As a summary of the preceding paragraphs, the following points need to be taken into account when designing the controller:

1. Robust compensation of the negative stiffness K_X (typically $K_P=2\cdot K_X$).
2. High damping of rigid body modes.
3. Damping greater than 20% for bending modes within the operational speed range.
4. Stability of the controlled system in the entire operational speed range.

To validate the feasibility of an AMB motor design during the concept phase and to identify a suitable controller parameterization required for commissioning, the closed-loop dynamics of the system need to be simulated beforehand, see Figure 15. This requires a thorough FEM modeling of the rotor dynamics and the actuator characteristics, as well as detailed models of the position and current controller and the transfer characteristics of the sensor.

These models are then fine-tuned by measuring the system dynamics during the commissioning phase to ensure that the rotor will manifest the same well-behaved behavior during run-up as predicted by the simulation.

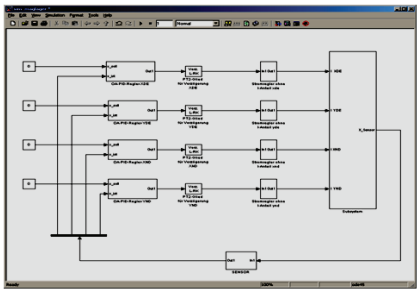

Figure 15: MATLAB/SIMULINK simulation model of the controlled rotor including position controller, current controller, sensor, bearing and rotor dynamics.

5 Test Bed with 5MW Induction Motor

The test bed for the AMB system based on standard drive technology is the high-speed induction motor with solid

shaft mentioned earlier. This motor has a rated power of 5MW at 13,500 rpm (225 Hz). The shaft weighs approximately 1.2t. The motor has been constructed as a supercritical motor, which will operate above the first bending mode and below the second bending mode. The test bed for AMB system based on standard drive technology with motor and control cabinet is shown in Figure 16 (left).

The simulated Campbell diagram of the closed-loop system for the final controller design is shown in Figure 16 (right). As indicated, the rigid body modes at 25 Hz are properly damped with 40% and 90%, respectively. The frequency of the first bending mode is shifted from 130Hz to 152Hz as a result of the controller action, while a damping of 30% was able to be realized, thus overachieving API requirements.

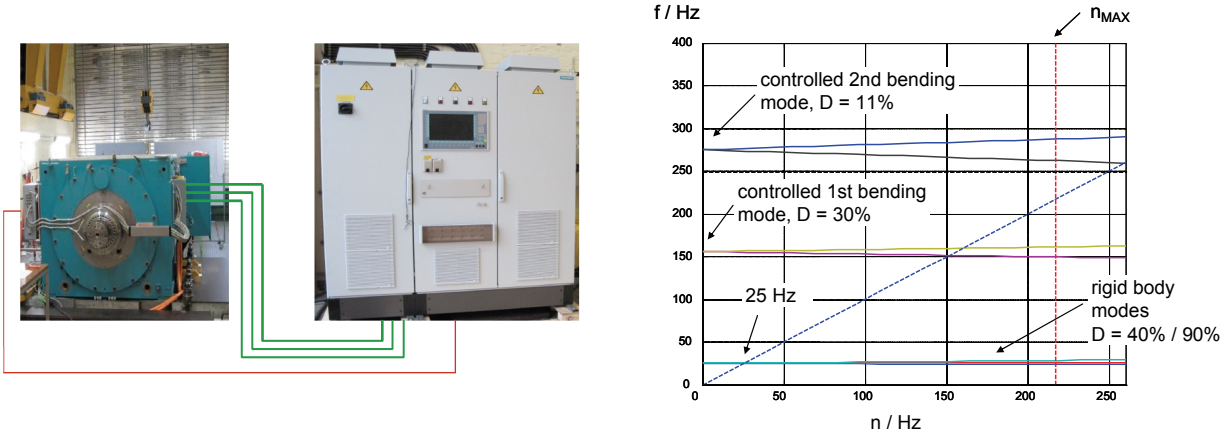

Figure 16: Test bed with 5 MW induction motor and controller cabinet (left). Campbell diagram for the closed-loop dynamics of the test motor with the final controller design (right).

A root locus analysis of the closed-loop controlled system, which shows the movement of the system poles over the operational speed range in the complex plane, is shown in Figure 17 (left). Because of the high damping, the poles of the 1st and 2nd bending mode lie outside the limits of the axes. The system is stable at all operating speeds as all poles remain on the left-hand side of the stability boundary.

The high-precision dynamic rotor balancing machine was not available while the rotor was being built, and it was only statically balanced. As a consequence, a significant dynamic unbalance was expected for the rotor, while the balancing documents indicate a high static balance quality. To study the effect of a dynamic unbalance on the run-up behavior, a run-up simulation with a dynamic unbalance of quality grade G2.5 was performed. For this purpose, two unbalance masses of 1144 gm each were introduced on opposite rotor sides in the antinodes of the second bending mode in the simulation. The simulation result is shown in Figure 17 (right). The simulation predicts a maximum of the vibration amplitudes (0-pk) at a speed of 160 Hz for the drive end, while the non-drive end vibration amplitude continues to rise with increasing velocity.

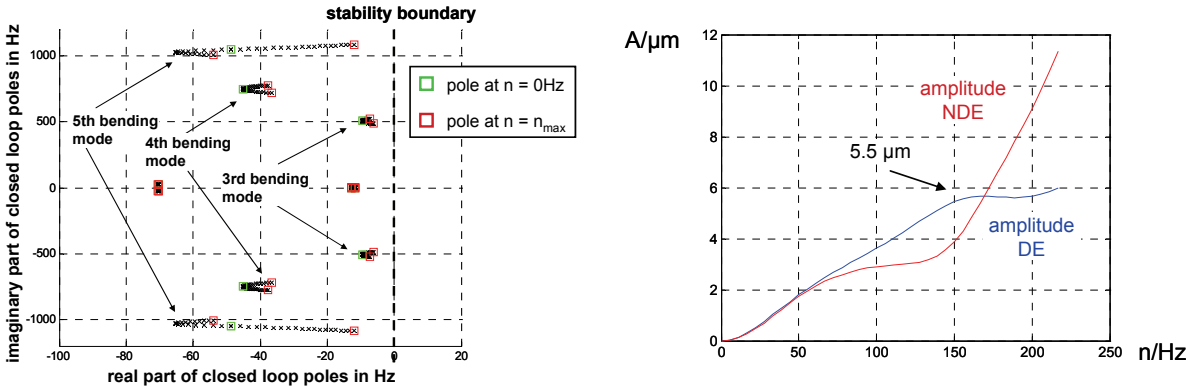

Figure 17: Root locus analysis: Poles of the controlled system for rotor speeds n= 0Hz ... 216Hz/13000rpm (left). Vibration amplitudes at sensor locations for unbalance simulation with a dynamic G2.5 unbalance (right).

6 Simplified AMB Commissioning using Standard Drive Technology Tools

Commissioning AMB systems is considerably simplified by employing the data acquisition function of standard drive technology equipment, embedded in a multi-axis drive control environment, just the same as for a numerical control system (NC). One of the basic functions of this type of system is the management and storage of the real-time data relating to position, current, voltage etc. This involves generating setpoints and acquiring actual values. Furthermore, the multi-axis drive control environment comprises optional data acquisition modules that are compatible to the system. These modules allow external signals, such as voltage signals or sine/cosine signals of electrical precision dial gauges to be read. This means that the signals of the external sensors can be recorded and processed together with the internal sensors, such as rotor position, current or voltage. The data management is enhanced by integrated analytical mathematical functions. The data that is collected can also be stored as ASCII tables, which can then be processed using external mathematical programs that can be freely selected.
Commissioning the 5MW test motor followed the nine steps as shown in Table I. This commissioning procedure is typical for all AMB systems regardless of whether they use standard drive technology or customized electronics. All of these steps are important and provide the commissioning engineer with important information about the actual system.

No.	Commissioning Step (CS)	each time	only for a prototype	with ext. meas. equip.	onboard equip. suff.icient	only by experts	AMB- service personnel
1	Measurement of the inductivity => correct size of air gap verified	x		x			x
2	Adjustment of the current control amplification		x		x		x
3	Identification of center of back-up bearing as position setpoint by pulling the rotor along the back-up bearing	x			x		x
4	Modal identification of the rotor in soft support with weakened magnetic force => rotor model verified	x			x		x
5	First levitation	x			x		x
6	Precision calibration of the position sensors when levitated using transverse movement => sensor gain verified		x		x		x
7	Determination of force to current ratio and destabilizing spring => magnetic bearing simulation model verified		x	x			x
8	Measurement of closed-loop position control transfer function / comparison to simulation => simulation model verified		x		x	x	
9	Documentation of shaft vibration amplitudes and bearing currents during run-up	x			x		x

Table 1: Commissioning steps (CS) for machines with AMB systems.

The procedure can be automated so that not only specifically trained AMB experts can work on the AMB system, but also commissioning personnel.

A few examples from the commissioning step table shown above are referred to in the following, which

highlight the advantages of the data management functionality integrated in standard drive technology when it comes to commissioning. These tools help to keep the commissioning time short. The steps mentioned in detail are 4, 6, 7 and 8. Steps 6 and 9 can also be used for checking the bearing during service and maintenance intervals of AMB machines as well as after an uncontrolled de-levitation of the rotor into the backup bearings.

From commissioning steps 1-7, all system parameters are known, which allows the simulation model to be fine-tuned. At the end of commissioning step 8, the closed-loop simulation model is verified by comparing simulation and measurement. The fine-tuned simulation model allows a final prediction of the behavior of the rotor during run-up. If the run-up behavior in simulation still shows the desired behavior, the rotor can be safely accelerated up to the rated speed of the motor during commissioning step 9.

6.1 CS 4: "Modal identification of rotor in soft support"

The modal identification of the rotor in soft support is performed before the rotor levitates. The purpose of this commissioning step is to validate the dynamic FE model of the rotor. To achieve this, the rotor is supported at both ends on soft supports, e.g. Teflon supports, at the center position of the back-up bearing, while the influence of the destabilizing stiffness is weakened by reducing the bias current in order to prevent the rotor from leaving or damaging the soft supports. The DE side of the rotor is then excited in one axis by generating colored current noise at the DE bearing with the commissioning tool of the standard drive system. The frequency response function can be calculated by recording the rotor position at the DE sensor and using the mathematical functions of the commissioning tool. The result is shown in blue in Figure 18. After including the respective frequency response function obtained from simulation (magenta), the correlation between the transfer functions can be assessed and the model can be adapted if the correlation is not adequate. In the example shown, for the resonances corresponding to the first four bending modes, there is a good correlation between simulation and reality, indicating a good modeling quality. After the DE, the same is done for the NDE. Since the support is soft enough, the transfer function is only influenced up to a frequency of about 100 Hz by the support stiffness.

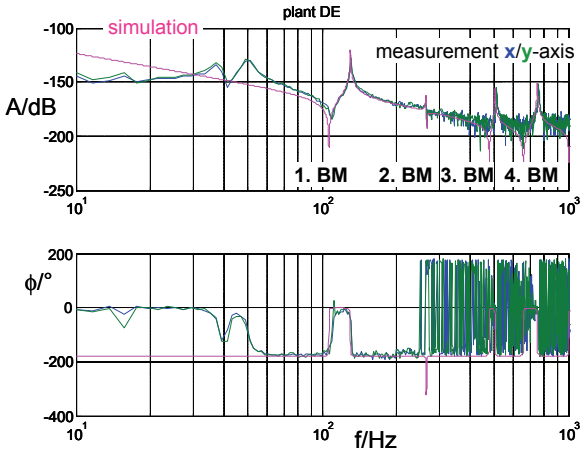

Figure 18: Transfer function of the DE position control plant in simulation and measurement up to the fourth bending mode (BM).

6.2 CS 6: "Calibration of position sensors"

Only contactless position sensors are permitted in AMB applications. Thus, their sensitivity must be calibrated with respect to an absolute reference if a high geometrical accuracy is required. A high sensor precision is especially useful when the rotor is to be used as a measurement tool over the motor service life to monitor the wear of adjacent surfaces – such as seals or back-up bearings. To measure the wear of adjacent surfaces, the rotor is moved between the surfaces according to a programmed motion profile and contact is detected by a non-linear change in bearing current.

The “Precision calibration of the position sensors when levitated using transverse movement” provides machine tool precision at AMB position coordinates. Two external electric dial gauges are attached to the motor as reference, one at each shaft end, see Figure 19. Dial gauges such as these are available as incremental scales with an accuracy of 0.01 µm. Their electrical sine/cosine interface to the drive is identical with the interface of the incremental position encoders of servomotors used in standard drive applications.

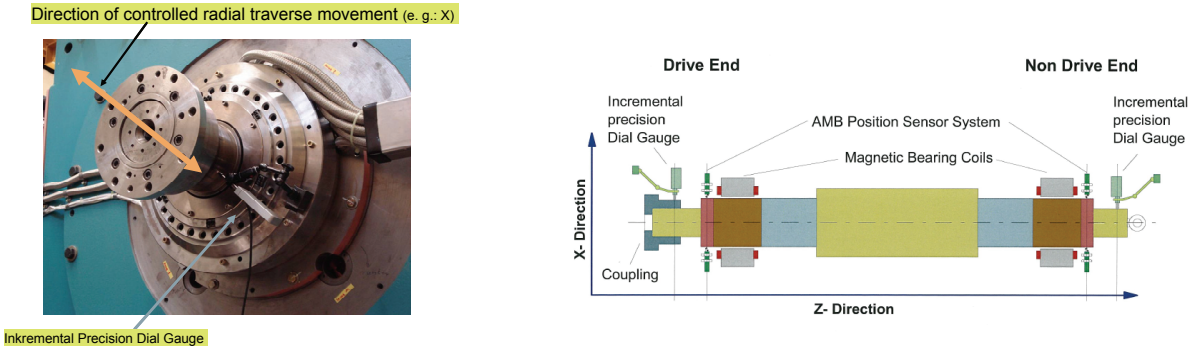

Figure 19: Applying transverse force to the rotor (left). Arrangement for sensor precision calibration (right).

While levitated, the numerical control (NC) functionality of the SIMOTION traverses the rotor within the backup bearing air gap. Both position traces, one for the internal AMB position measurement system itself and the other one for the external reference, are displayed in the same diagram, see Figure 20.

In the depicted example, the desired length of the numerically-controlled motion was 80 µm. In the non-calibrated state, the length of travel monitored by the reference dial gauges, does not perfectly correlate with the controlled one. The ratio between both lengths of travel exactly yields the scaling factor, which should be entered into the machine data for compensation. Figure 20 shows the measurement after compensation, in which the desired length of travel exactly matches the reference, i.e. there is only an offset between the two measurements.

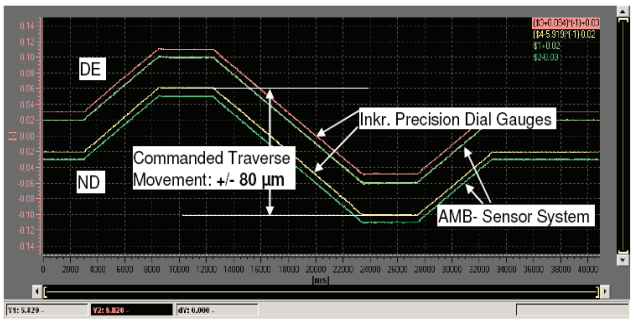

Figure 20: Diagram comparing the position measurement with the internal and external sensors.

6.3 CS 7: “Measurement of current-to-force constant”

The next example shows the precise measurement of the current-to-force ratio of the magnetic circuit. Here, the ability to read external +/-10 V signals with the standard drive makes the measurement easy to perform and minimizes the amount of equipment required. The principle of the measurement is to apply an external force in the form of a ramp function to the rotor and to measure the change of bearing current due to the applied force. The rotor is in controlled levitation. Therefore, the applied force is balanced entirely by the active magnetic bearing current and a force to current relation is obtained. The external force ramp is generated using a mechanical spring, which is pulled using a crane, see Figure 21 (left), while the magnitude of the external force is measured using a force measurement device. The +/- 10V output signal of the force measurement device is recorded with the drive system. This approach allows a complete current-to-force curve to be measured in one operation for one position setpoint of

the rotor – and not just a few points along the characteristic.

Because one measurement run does not involve much time, it is possible to move the rotor to several position setpoints in the air gap. This allows the field of characteristic curves of the bearing to be obtained, see Figure 21 (right). The rotor was positioned in steps of 20 µm within the air gap. Each curve represents the force-to-current characteristic of the particular position. The data was traced and stored in the multi-axis drive control, and then saved in an ASCII table.

The force-to-current ratio exhibited good linearity. The non-linear component is negligible. Good linearity is desired in order to achieve a control behavior independent of the load. When the position setpoint is moved, the force-to-current curve is shifted in parallel by a certain amount, but the slope remains unchanged. The slope directly represents the force per control current ratio. In this case, it is 516 N/A. It is independent of the position. Achieving the same control behavior at each rotor position in the back-up bearing gap is also a desirable aspect of the AMB design. The parallel shift of the force-to-current curve by the position is the result of the destabilizing magnetic force discussed before. The evaluation of the destabilizing stiffness from the field of characteristic curves yielded a value of 15.4 N/µm.

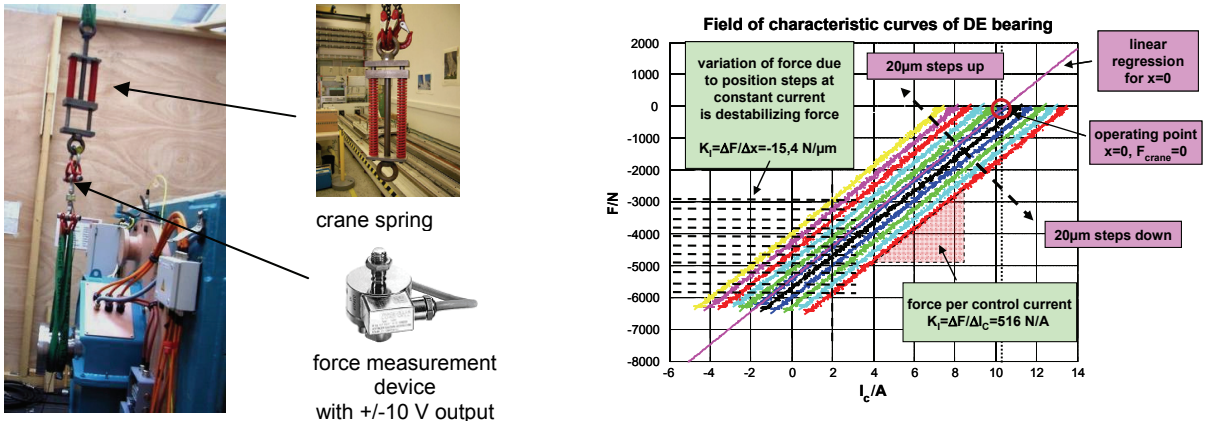

Figure 21: Arrangement for generating a force ramp by lifting with a crane (left). Diagram showing the current-to-force curves at several different position setpoints (right).

6.4 CS 8: "Measurement of closed-loop position control transfer function"

Comparisons between simulated system transfer functions and the system transfer functions that are measured using the measuring functions, which are implemented in the commissioning software of the standard drives, show a good correlation between simulation and reality, see example in Figure 22. After this commissioning step, it can be concluded that in reality, the rotor will show the same qualitative behavior during run-up as indicated by simulation.

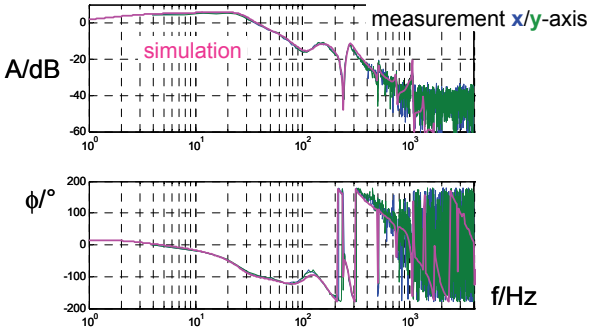

Figure 22: Transfer function of the closed-loop controller in simulation and measurement.

7 Test Results From a Run-Up

The motor was accelerated successfully up to 10,000 rpm. This is higher than the first bending mode, see Figure 23. The vibration levels at the bearing housing and the orbits of the rotor in the AMB were observed during run up. When the first bending mode is passed through, this is barely visible due to the high damping realized by the AMB. At 25Hz, the rigid body modes are excited, possibly by eccentricity between actuator or sensor target area and rotor axis. As expected, the unbalance response behavior is qualitatively very similar to that in Figure 17 (right) for higher speeds. However, as indicated by the higher vibration amplitudes, the balance quality of the rotor is worse than that obtained from the simulation.

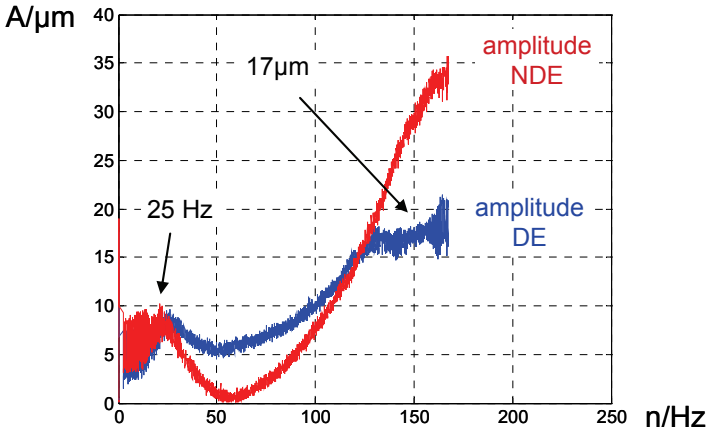

Figure 23: Run-up to 167Hz / 10,000 rpm. Orbit at DE and NDE recorded with onboard tools (rigid body modes at 25 Hz, 1st bending frequency of the free rotor at 130 Hz, damped 1st bending frequency of the controlled rotor at 154 Hz).

8 Conclusion

The successful prototype testing results presented in this paper show that standard drive controllers and power modules – of which more than 100,000 units are built per year – can be applied to operate active magnetic bearings in large motor applications. To achieve this, only software modifications in the drive components are required. The available interfaces of the standard drive technology and the commissioning functionality implemented in the engineering system of the standard drive technology significantly simplify the commissioning process. We are positive that this technology can help to further build up customer confidence and therefore increase the use of active magnetic bearing technology in turbomachinery applications.

References

[1] E. Schäfers, J. Denk and J. Hamann, “Mechatronic Design of Direct Drive Systems“, in *International Symposium on Power Electronics, Electrical Drives, Automation and Motion, (SPEEDAM 2006)*, 2006, pp. 1051-1055.

[2] C. Gähler, *“Rotor dynamic testing and control with active magnetic bearing”* , PhD Thesis, Zürich, Switzerland, Swiss Federal Institute of Technology, 1998.

[3] API Standard 617, *"Axial and Centrifugal Compressors and Expander-compressors for the Petroleum Chemical and Gas Industry"*, Seventh Edition, 2002.

A Nomenclature

a	acceleration (m/s²)
A	amplitude of transfer function (dB) or vibration (m)
f	frequency (Hz)
f_C	controller action force (N)
F	Force (N)
F_g	gravitational force (N)
i_d	flux current (A)
i_q	torque current (A)
i_R	current phase R (A)
i_S	current phase S (A)
i_T	current phase T (A)
I_C	control current (A)
I_0	bias current (A)
I_1	current upper coil (A)
I_2	current lower coil (A)
k	constant
K_I	force per control current (N/A)
K_P	proportional gain of controller (N/m)
K_X	force per displacement (N/m)
M	mass (kg)
n	rotational speed (rev. per second)
R	rotor radius (m)
ΔR	rotor growth (m)
s	derivative (1/s)
1/s	integral (s)
T_N	integral action of controller (s)
T_V	derivative action of controller (s)
v	velocity (m/s)
x	position, displacement (m)
x_A	position signal sensor A (m)
x_B	position signal sensor B (m)
x_0	gap for centered rotor (m)
x_{sense}	position signal (m)
x_S	set point position (m)
z	disturbance (N)
Φ	phase of transfer function (°)